

DEVELOPING REGIONALIZED MODELS OF LITHOSPHERIC THICKNESS AND VELOCITY STRUCTURE ACROSS EURASIA AND THE MIDDLE EAST FROM JOINTLY INVERTING P-WAVE AND S-WAVE RECEIVER FUNCTIONS WITH RAYLEIGH WAVE GROUP AND PHASE VELOCITIES

Jordi Julià¹, Eric Matzel², Andrew A. Nyblade¹, and Arthur J. Rodgers²

Penn State University¹ and Lawrence Livermore National Laboratory²

Sponsored by the National Nuclear Security Administration

Award Nos. DE-AC52-09NA29322¹ and DE-AC52-07NA27344²

Proposal No. BAA09-13

ABSTRACT

The main goal of this project is to develop models of lithospheric velocity structure for Eurasia and the Middle East in order to improve capabilities within National Nuclear Security Administration (NNSA) labs to accurately predict travel times for local and regional phases, as well as travel-times for body waves at upper-mantle triplication distances. Velocity models of the lithosphere are key for accurately modeling not only travel times but also surface-wave dispersion velocities and full waveforms at regional (2°–15°) and far-regional (15°–25°) distances. The models are being developed following a two-step approach: first, one-dimensional (1D) velocity models for select broadband stations are obtained by jointly inverting P- and S-wave receiver functions and fundamental-mode group and phase dispersion velocities; second, regionalized velocity models are constructed by combining the 1D joint inversion models within regions used in the UNIFIED model and are validated through regional waveform modeling. We expect the velocity models will also help inform and strengthen ongoing and future efforts within the NNSA labs to develop three-dimensional (3D) velocity models for Eurasia and the Middle East, assist in obtaining model-based predictions where no empirical data are available, and improve event locations in regions with sparse network coverage.

So far, we have obtained a total of 59 joint inversion models in Eurasia and the Middle East: 35 for Europe, 10 for the Middle East, and 14 for Asia. To develop these models, we have considered permanent broadband stations with open access and with waveforms archived at the Data Management Center (DMC) of the Incorporated Research Institutes for Seismology (IRIS). The station distribution is quite uneven among the UNIFIED regions, and the selected stations have been complemented with open stations archived at other data centers when available. P-wave receiver functions have been computed for all the selected stations at overlapping frequency bands of $f < 0.5$ Hz and $f < 1.25$ Hz, totaling 78,267 in the low-frequency band and 80,218 in the high-frequency band. S-wave receiver functions have been computed for $f < 0.5$ Hz, totaling 5,868. And fundamental-mode, Rayleigh-wave, group velocities have been obtained from an independent surface-wave tomography study for Eurasia and North Africa, for periods between 10 and 100 s. The velocity models obtained from the joint inversion of these datasets reveal important differences in lithospheric structure among UNIFIED regions. In the cratonic regions of eastern Europe, no sharp velocity decrease is observed down to ~250 km depth, while in the tectonic regions of western Europe and the Middle East, low-velocity zones in the lithospheric mantle are common. In the cratonic areas of Asia, on the other hand, some stations do display well-defined low-velocity channels within the lithosphere.

We have also developed regionalized velocity models for UNIFIED regions in Europe and the Middle East. The models have been constructed after combining 1D velocity models from the joint inversion of P- and S-wave receiver functions and dispersion velocities within the regions. The regionalized models have been verified by modeling regional waveforms from the Seismic Research Database of the Lawrence Livermore National Laboratory (LLNL) Ground-Based Nuclear Explosion Monitoring (GNEM) Research and Development program for events with well-determined source parameters and ray-paths predominately within the UNIFIED region. The validation exercise reveals that the body-wave portion of the regional waveforms is correctly predicted by the regionalized models, but the surface-wave portion requires modification. We are now investigating why models constrained by teleseismic surface-wave dispersion velocities are not capable of predicting regional surface-wave phases and amplitudes.

OBJECTIVES

The main objective of this project is to develop models of lithospheric thickness and velocity structure for a wide variety of tectonic regions throughout Eurasia and the Middle East. The new models will improve NNSA labs' abilities to accurately predict travel times for local and regional phases, such as Pg, Pn, Sn, and Lg, as well as travel times for body waves at upper-mantle triplication distances. They will also help inform and strengthen ongoing and future efforts to develop 3D velocity models for Eurasia and the Middle East. It is important that the new velocity models will assist in obtaining model-based predictions where no empirical data are available (e.g., Flanagan et al., 2006), and in improving locations from sparse networks (e.g., Schultz et al., 1998; Myers and Schultz, 2000).

The new velocity models are being developed through a two-step approach. In the first step, local velocity-depth profiles are obtained by jointly inverting up to three different seismic datasets: (1) P-wave receiver functions (PRFs), (2) S-wave receiver functions (SRFs), and (3) fundamental-mode Rayleigh-wave group velocities. In the second step, regionalized 1D velocity models are developed after the averaging of joint inversion models within tectonic regions of Eurasia and the Middle East. PRFs constrain detailed crust and uppermost-mantle velocity variations through S-P travel times and velocity contrast across discontinuities. SRFs constrain detailed lithospheric mantle structure, including lithospheric thickness, through P-S travel times and velocity contrasts across discontinuities. And surface-wave group velocities constrain large-scale average velocity structure at frequency-dependent depth ranges across the crust and upper mantle. All three datasets are sensitive mainly to S-wave velocity and provide complementary sets of constraints that bridge resolution gaps among them. The joint inversion approach integrates those constraints, producing S-wave velocity-depth profiles with the high-resolution details constrained by the receiver functions superimposed to an average background velocity model constrained by the surface-wave dispersion velocities (Julià et al., 2000).

The regionalized models are evaluated by comparing synthetic seismograms to data from events with well-determined source parameters (depth, seismic moment, and focal mechanism) and with ray-paths predominately within a single geologic/tectonic region. The model validation effort focuses on regions where there is good event-station coverage (i.e., pure path propagation through a region) over a range of local and regional distances. Using synthetics, we calculate how well the model reproduces the amplitude and phase of the data. By perturbing individual model elements, we create a sensitivity matrix for inversion. These data are highly sensitive to the crustal and uppermost-mantle shear velocity structure. For larger regions we focus on modeling body waves (Pn and upper mantle triplication P- and S-waves). Pn waveforms are most sensitive to crustal P-wave structure through the shear-coupled P-wave (PL) and lithospheric thickness, velocities, and velocity gradient through the timing and amplitude of the first-arriving P-wave (Pn). The timing and amplitude of triplications in the data are sensitive to lithospheric structure.

The tectonic regions for which regionalized velocity models are being produced are outlined in Figure 1 and correspond to the regions proposed in the UNIFIED model of Pasyanos et al. (2003; 2004). The UNIFIED models were constructed from *a priori* information in the published literature, and they subdivide Eurasia and the Middle East into tectonically distinct regions, each of which is characterized by multiple sediment, crustal, and upper-mantle layers with specified thicknesses, compressional and shear velocities, densities, and attenuation factors (Pasyanos et al., 2003; 2004). Our "regionalized" velocity models will characterize the average structure within the same tectonic regions and will include estimates of lithospheric thickness, velocity structure of the lithospheric mantle, and structure of the low-velocity zone beneath the lithospheric lid.

The regionalized velocity models developed for the UNIFIED regions will aid ongoing efforts to develop 3D velocity models for Eurasia and the Middle East, such as the Seismic Lithosphere Base Model (SLBM). In the SLBM models, each point is parameterized as a crust with variable velocity and thickness over a mantle half-space with a constant sub-Moho velocity and velocity gradient. Because the mantle lithosphere is parameterized as infinitely thick with a constant velocity gradient, the model cannot accurately model rays that penetrate below the lithosphere. As such the current SLBM is limited, and cannot be used for travel-time predictions or waveform modeling much beyond a distance of about 12°. The new models will add the necessary details about the velocity structure of the lithospheric mantle, the thickness of the lithosphere, and the structure of the low-velocity zone under

the lithosphere to extend prediction and modeling capabilities beyond 12°.

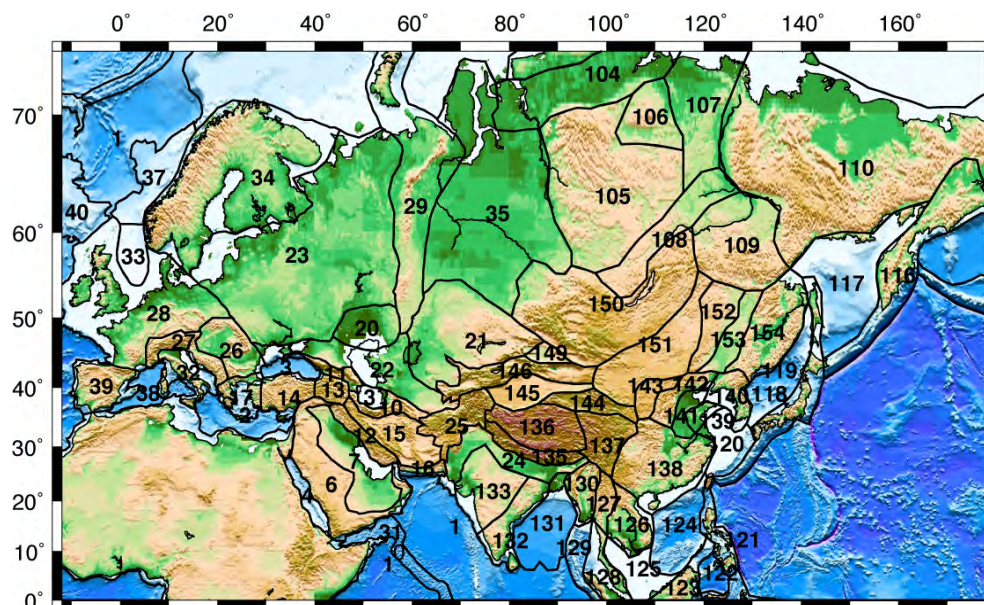


Figure 1. The UNIFIED model, with contributions from both LLNL and Los Alamos National Laboratory (LANL). The numbered areas mark tectonically distinct regions defined by Pasyanos et al. (2003; 2004).

RESEARCH ACCOMPLISHED

We have now completed the gathering of teleseismic P- and S-waveforms at open broadband stations in Eurasia and the Middle East as well as the computation of PRFs and SRFs from the collected waveforms. We have also completed the development of joint inversion models for Europe and the Middle East and are now completing the development of joint inversion models for Asia. Regionalized models for UNIFIED regions in Europe and the Middle East are being developed from the joint inversion models developed during the first year.

Data Gathering

During the second year of application of this project, we completed the gathering of teleseismic P- and S-waveforms for the computation of PRFs and SRFs in Asia. The dataset consists of 226,584 P-waveforms in the $30^\circ < \Delta < 90^\circ$ distance range and magnitude above 5.5 and 51,124 S-waveforms corresponding to events in the $60^\circ < \Delta < 82^\circ$ distance range and magnitude above 5.7, as recorded at 143 open broadband stations in the region (Figure 2). The waveforms have been downloaded from the IRIS archive using the Standard Order for Data (SOD) utility of Owens et al. (2004).

Fundamental-mode Rayleigh-wave group velocities in Europe and the Middle East were obtained from the surface-wave tomography study of Pasyanos (2005). In that study, local dispersion curves were obtained for Eurasia, the Middle East, and North Africa by inverting fundamental-mode Rayleigh-wave group velocities measured along more than 30,000 source-station paths with a conjugate-gradient method with variable smoothness. The resulting surface-wave tomography maps highlight lateral variations across the region for periods between 7 and 100 s with a resolution approaching 1° .

A number of regional events with well-determined source parameters and ray-paths predominately contained within terranes defined in the UNIFIED models have been identified for Europe and the Middle East. The events have large signal-to-noise ratios and are well recorded at the seismic stations. The terranes sampled by the 1D joint inversion models include regions number 06, 13, 14, 22, 23, 26, 27, 28, 29, 32, 34 and 39 (Figure 1). The regional waveforms

were selected from the Seismic Research Database of the LLNL GNEM program and will be utilized to evaluate the average velocity models that will be developed for the geologic/tectonic terrains from the local 1D models.

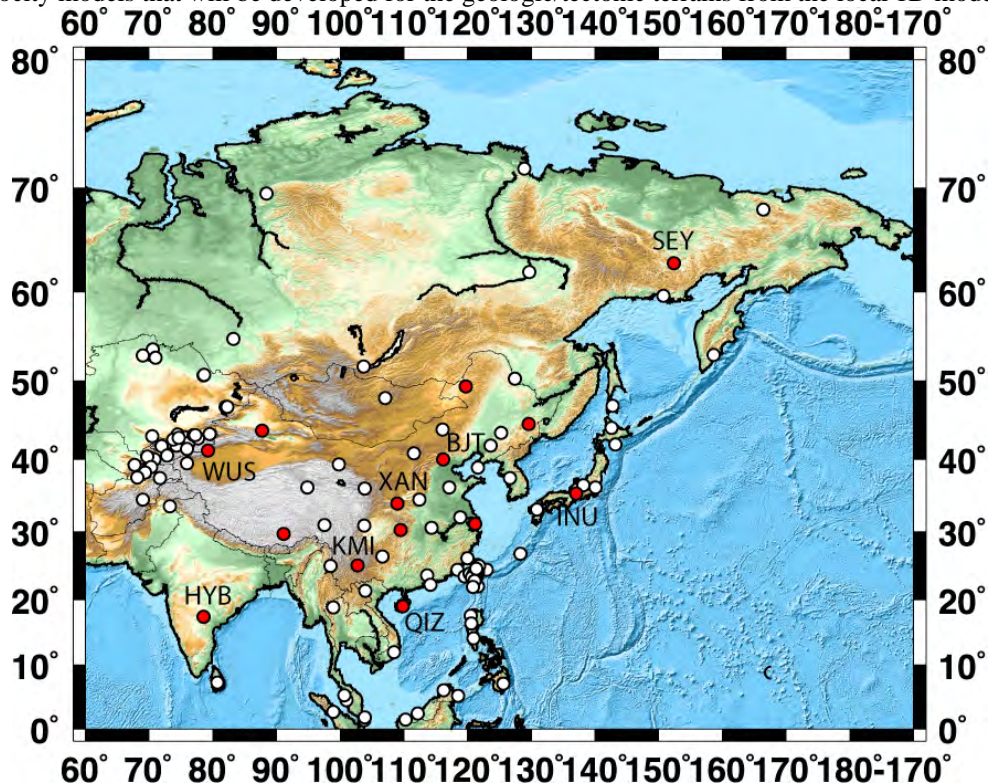


Figure 2. Topographic map of Asia showing the 143 permanent broadband stations (white circles) considered in this work. Some stations overlap and will be combined for a single estimate of the 1D velocity models with the joint inversion procedure. The red circles denote stations for which a joint inversion model has been developed.

Receiver Function Computation

During the second year of application, we also completed the computation of PRFs for selected permanent broadband stations in Asia (Figure 2). The PRFs were obtained in the ZRT coordinate system by deconvolving the vertical component of the teleseismic P-waveforms from the corresponding radial component, using the iterative time-domain procedure of Ligorria and Ammon (1999), with 500 iterations. PRFs were computed at two overlapping frequency bands of $f < 1.2$ Hz and $f < 0.5$ Hz. A first-pass quality control was applied to the PRFs by convolving them back with the corresponding vertical component and comparing predicted and observed radial waveforms. Only those reproducing at least 85% of the original radial component were selected, yielding a total of 9,145 PRFs for the high-frequency band and 9,537 PRFs for the low-frequency band.

We have also completed the computation of SRFs for the same selection of permanent broadband stations. Following standard SRF computation practices (e.g. Hansen et al., 2007), SRFs have been obtained in the local ray-coordinate system after deconvolving the Q component (SV-wave) of teleseismic S-waveforms from the corresponding L component (P-wave). The deconvolution has been performed through the iterative time-domain procedure of Ligorria and Ammon (1999), with 500 iterations, after low-pass filtering below 0.5 Hz. Similar to PRFs, a first-pass quality control has been applied to the computed SRFs by convolving them back with the corresponding L component and comparing predicted and observed waveforms. Only those reproducing at least 85% of the original radial component have been selected, yielding a total of 5,579 SRFs. This number will likely be reduced after visual inspection of the selected SRF waveforms.

The receiver function computation effort (for both PRFs and SRFs) in Eurasia and the Middle East has thus been finalized. Additional stations with open data access from other data centers might be included in the future in order

to improve the sampling of UNIFIED regions with little data coverage from the IRIS-Data Management Center database.

Development of Joint Inversion Models

During the second year of application, we started the development of 1D S-velocity models from the joint inversion of PRFs, SRFs, and group velocities at broadband stations in Asia. We concentrated on permanent broadband stations with operating times of over 5 years in order to develop robust receiver function averages and be able to inspect for azimuthal variations around the station. Using large datasets is especially important for obtaining reliable SRF estimates, as events must be within epicentral distance ranges that are narrower than those for PRFs (Wilson et al., 2006), and the deconvolution process is more unstable. Overall, we developed 14 joint inversion models in Asia.

The joint inversion procedure utilized follows the iterative, linearized approach of Julià et al. (2003). The approach is described by the following system of equations:

$$\begin{bmatrix} \sqrt{\frac{p}{w_s^2}} D_s \\ \sqrt{\frac{q}{w_b^2}} D_b \\ \sigma \Delta \\ A \end{bmatrix} \vec{m} = \begin{bmatrix} \sqrt{\frac{p}{w_s^2}} \vec{r}_s \\ \sqrt{\frac{q}{w_b^2}} \vec{r}_b \\ \vec{0} \\ A \vec{m}_a \end{bmatrix} + \begin{bmatrix} \sqrt{\frac{p}{w_s^2}} D_s \\ \sqrt{\frac{q}{w_b^2}} D_b \\ \vec{0} \\ \vec{0} \end{bmatrix} \vec{m}_0$$

where D_s and D_b are partial derivative matrices for the dispersion and the receiver function estimates, respectively, r_s and r_b are the corresponding vectors of residuals, w_s^2 and w_b^2 are weights that equalize the datasets, the vector m contains the velocities of fixed-thickness layers overlying a half-space, and m_0 contains an initial estimate for the velocities. The matrix Δ constructs the second difference model and makes the resulting profiles vary smoothly, and the diagonal matrix W contains constraint weights to the *a priori* velocity values m_a . The influence factor p controls the trade-off between fitting the receiver functions and the dispersion curves, and the smoothness parameter σ controls the trade-off between fitting the data and model smoothness. The parameter $q = 1-p$, with $0 \leq p \leq 1$, so that $p = 0$ means inverting receiver function data only, and $p = 1$ means inverting dispersion data only. The weights w_s^2 and w_b^2 were computed as $N\sigma^2$, where N is the number of data points and σ^2 is the variance of the observations, to account for differences in the number of data points and physical units.

Figure 3 displays an example at station XAN, located in UNIFIED region #143 (Figure 1). PRFs and SRFs were grouped by back-azimuth and ray parameter (or, equivalently, incidence angle) before the inversion, in order to investigate lateral variations in velocity structure around the recording station. The influence factor was given a value of $p = 0.5$ so that each dataset contributes similarly to the combined L2 misfit function, and the smoothness parameter was chosen to provide the highest resolution possible while keeping the inversion stable. Velocities below ~250 km depth were constrained to be PREM-like (Dziewonski and Anderson, 1981) to account for the partial sensitivity of long-period dispersion velocities to deeper structure. The resulting velocity model is simple and displays a 38–40-km-thick crust, consisting of an 8–10-km-thick upper crust with S-velocity around 3.1 km/s and a ~30-km-thick lower crust with uniform S-velocity of ~3.7 km/s down to 30 km depth, overlying a sharp gradational increase up to 4.5 km/s at Moho depths. The mantle is PREM-like and does not display any velocity decrease suggestive of a lithosphere-asthenosphere boundary (LAB). The inverted model satisfactorily predicts the dispersion velocities and the main features in the receiver function waveforms. Nonetheless, some secondary arrivals in the high-frequency PRFs are not matched, and the amplitudes in one of the SRF waveforms are clearly underestimated. We think this is the result of lateral variations of Earth structure around the station, as station XAN is located near the boundaries of UNIFIED regions #144 and #151.

Figure 4 displays a subset of the joint inversion models developed in Asia, corresponding to those under stations operated by the French GEOSCOPE global network and the new China Digital Seismographic Network (CDSN). Crustal thicknesses range from 32 km under station HYB to more than 50 km under station WUS, in good agreement with independent studies (e.g., Chen et al., 2010). The lithospheric structure, as revealed by the computed

SRF waveforms, generally includes a velocity drop at depths around 100 km or shallower; this velocity drop might correspond to the LAB or some other intra-lithospheric discontinuity (e.g., Rychert et al., 2009). Under stations HYB and KMI, however, no clear seismic discontinuities are imaged in the lithospheric mantle.

These results contrast with the findings reported last year for Europe, where consistent differences in lithospheric structure were observed between the East European craton and Phanerozoic Western Europe. The lithosphere under East Europe was characterized by the lack of a sharp velocity decrease above the 250-km depth that could mark the location of the LAB, while the lithosphere under Western Europe was rich in seismic discontinuities that could be interpreted as the boundaries of a low-velocity channel. These two types of structures are observed for the Asian lithosphere, but their correlation with continental age is less clear.

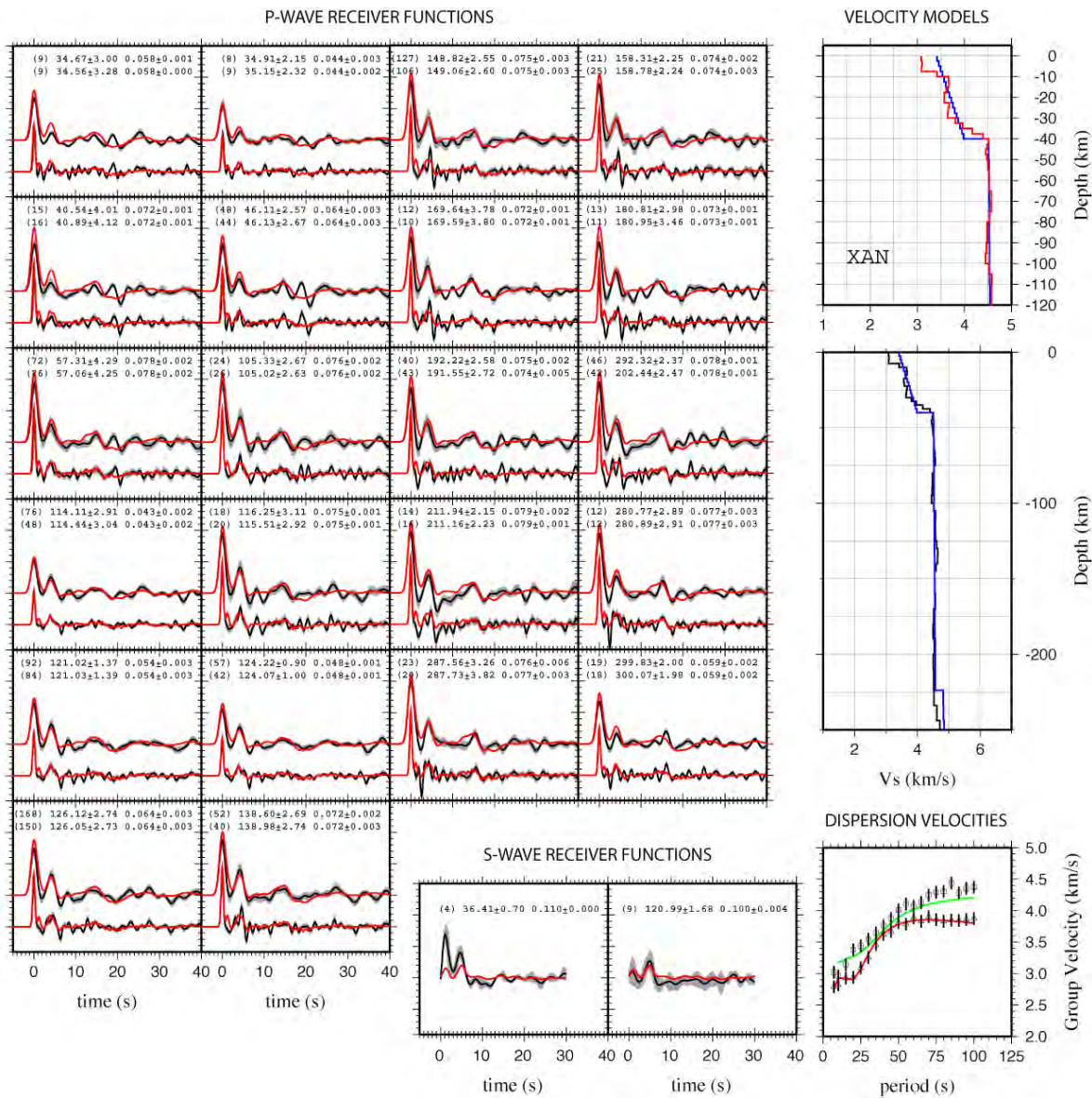


Figure 3. Joint inversion results for station XAN, China. Each PRF and SRF panel contains receiver function averages for the back-azimuth and ray-parameter values noted on top. The number of waveforms contributing to the average stack is noted in parentheses. Observations and predictions are represented in the receiver function panels by black and red lines, respectively, and in the group velocity panel by triangles and red lines, respectively. The velocity models for the crust and lithosphere are shown to the right.

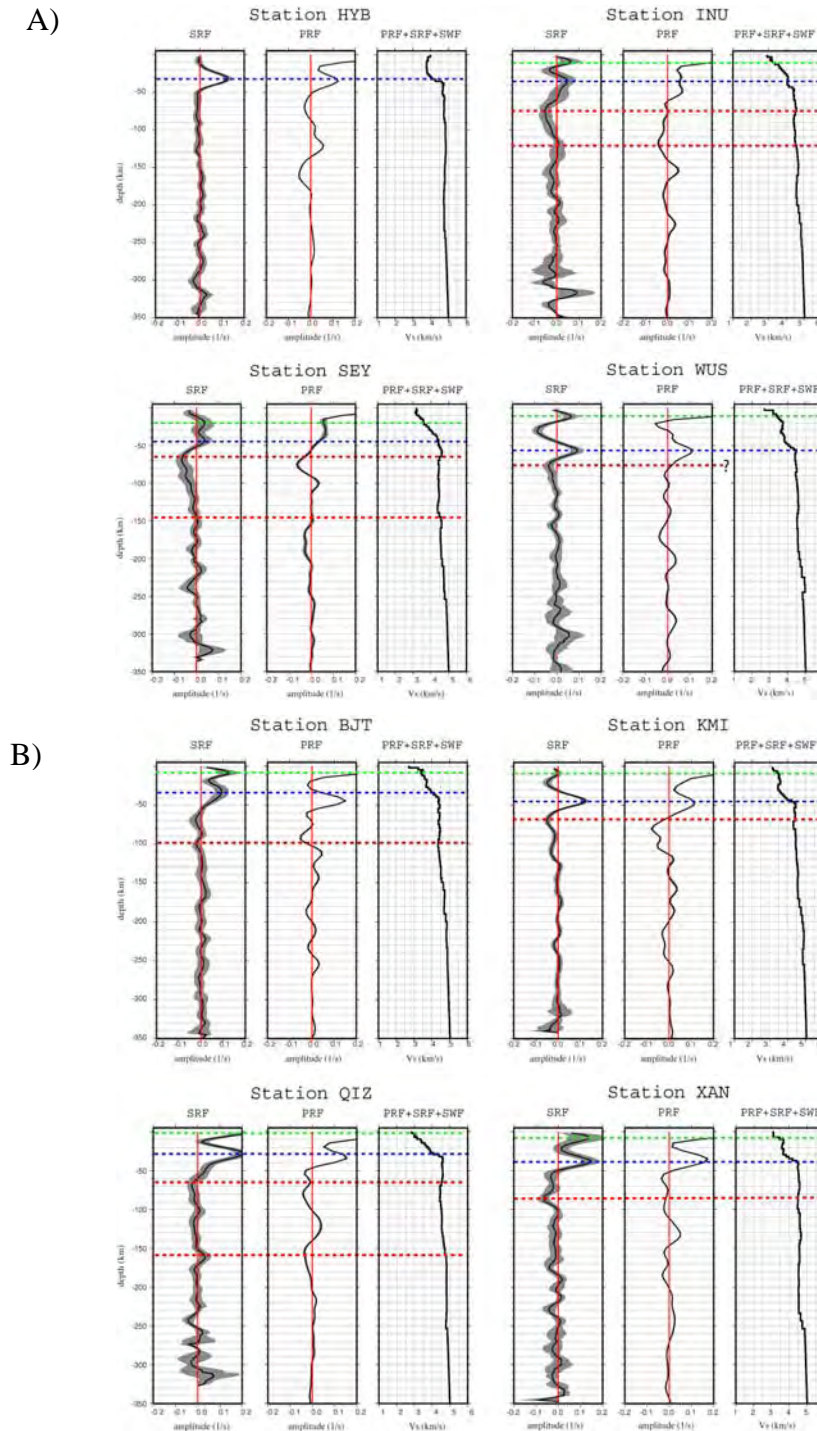


Figure 4. Joint inversion results for GEOSCOPE (A) and CDSN (B) stations in Asia. The PRF and SRF waveforms have been migrated to depth using the ak135 earth model to allow for a better comparison to the velocity-depth profiles. The models were inverted down to a depth of 250 km and constrained to be PREM below. The low-velocity channel is bounded by the red dotted lines, the Moho is marked by the blue dotted line, and some intra-crustal discontinuities are marked by green dotted lines.

Development of Regionalized Models

We have also begun developing regionalized models for the UNIFIED regions (Pasyanos et al., 2003) in Europe and the Middle East by combining the joint inversion models developed during the first year of this project. As a first step, the joint inversion models within each UNIFIED region were tested through modeling of regional waveforms with ray-paths within UNIFIED regions. **Figure 5** displays the results for an event with waveforms recorded at stations in and around Turkey (UNIFIED region #14). The joint inversion models do a good job matching the timing and amplitude of the body-wave arrivals, but the surface wave trains are more poorly fit. Figure 5 also shows that fitting the full waveforms requires significant changes in the lower crustal structure.

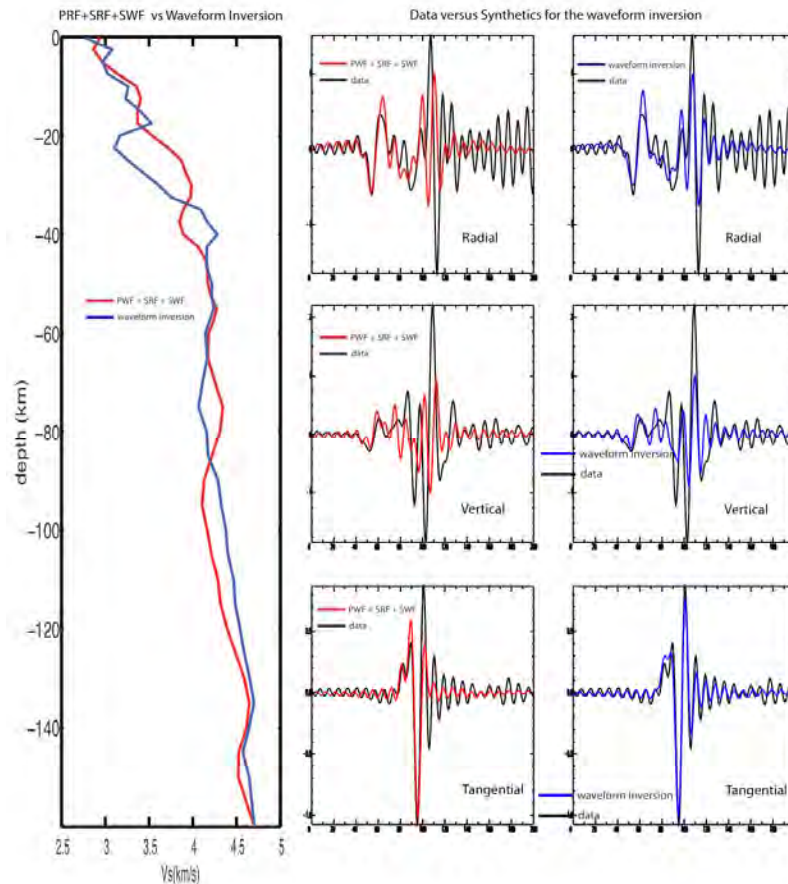


Figure 5. Forward modeling of regional waveforms at station ANTO, in UNIFIED region #14. The velocity models (left) and the corresponding predictions (middle and right) are shown in red for the joint inversion and in blue for the regional modeling. The joint inversion model satisfactorily matches the body-wave train but needs modification to produce a similar match to the surface-wave train. The synthetic seismograms were computed with the reflectivity method (Randall, 1994; Zhu and Rivera, 2002).

CONCLUSIONS AND RECOMMENDATIONS

We have completed the development of 1D joint inversion models for open broadband stations in Europe and the Middle East and are now completing the development of joint inversion models for open broadband stations in Asia. Overall, we have developed 59 joint inversion models: 35 for Europe, 10 for the Middle East, and 14 for Asia. Our results show that, as anticipated, SRFs control the location of seismic discontinuities in the lithospheric mantle and that the joint inversion models provide a more satisfactory representation of the lithospheric and sub-lithospheric mantle than do the existing UNIFIED and/or SLBM velocity models.

The development of new average 1D models from the joint inversion models for the UNIFIED regions in Eurasia and the Middle East has now started. The first step has been the validation of the joint inversion models through regional waveform modeling. Preliminary results in UNIFIED region #14 have shown that the joint inversion models cannot correctly predict surface-wave amplitudes for regional events. We suspect that crustal and lithospheric heterogeneity within the UNIFIED region, which favors distortion of the surface-wave train by multi-pathing effects, is most likely responsible. Average 1D models can still be developed for surface-wave propagation at low frequencies, but modeling of higher frequencies will likely require accounting for 3D structures.

ACKNOWLEDGEMENTS

We would like to thank the IRIS DMC and GEOFON Data Center for their role in the archiving and distribution of seismic data utilized for this project.

REFERENCES

- Chen, Y. L., F. L. Niu, R. F. Liu, Z. B. Huang, H. Tkalcic, L. Sun, and W. Chan (2010). Crustal structure beneath China from receiver function analysis, *J. Geophys. Res.* 115: B03307, doi:10.1029/2009JB006386.
- Dziewonski, A. M. and D. L. Anderson (1981). Preliminary reference Earth model, *Phys. Earth Planet. Inter.* 25: 297–356.
- Flanagan, M., S. Myers, and K. Koper (2006). Regional travel-time uncertainty and seismic location improvement using a three-dimensional a priori velocity model, *EOS Trans. AGU* 87: S31B-0194.
- Hansen, S., A. Rodgers, S. Schwartz, and A. Al-Amri (2007). Imaging ruptured lithosphere beneath the Red Sea and Arabian Peninsula, *Earth Planet. Sci. Lett.* 259: 256–265.
- Julià, J., C. J. Ammon, R. B. Herrmann, and A. M. Correig (2000). Joint inversion of receiver function and surface wave dispersion observations, *Geophys. J. Int.* 143: 99–112.
- Julià, J., C. Ammon, and R. Herrmann (2003). Lithospheric structure of the Arabian Shield from the joint inversion of receiver functions and surface-wave group velocities, *Tectonophysics* 371: 1–21.
- Ligorria, J. and C. Ammon (1999). Poisson's ratio variations of the crust beneath North America, *Seism. Res. Lett.*, 89: 1395–1400.
- Myers, S. and C. Schultz (2000). Improving sparse network seismic location with Bayesian kriging and teleseismically constrained calibration events, *Bull. Seismol. Soc. Am.* 90: 199–211.
- Owens, T. J., H. P. Crotwell, C. Groves, and P. Oliver-Paul (2004). Standing order for data, *Seism. Res. Lett.* 75: 515–520.
- Pasyanos, M., W. Walter, and M. Flanagan (2003). Geophysical models for nuclear explosion monitoring, in *Proceedings of the 25th Seismic Research Review—Nuclear Explosion Monitoring: Building the Knowledge Base*, :A-UR-03-6029, Vol. 1, pp. 125–134.
- Pasyanos, M., W. Walter, M. Flanagan, P. Goldstein, and J. Bhattacharyya (2004). Building and Testing an a priori geophysical model for western Eurasia and North America, *Pure Appl. Geophys* 161: 235-281.
- Pasyanos, M. (2005). A variable resolution surface wave dispersion study of Eurasia, North Africa, and surrounding regions, *J. Geophys. Res.* 110: doi: 10.1029/2005JB003749.
- Randall, G. (1994). Efficient calculation of complete differential seismograms for laterally homogeneous earth models, *Geophys. J. Int.* 118: 245–254.
- Rychert, C. A. and P. M. Shearer (2009). A global view of the lithosphere-asthenosphere boundary, *Science* 324: 495–498.

2011 Monitoring Research Review: Ground-Based Nuclear Explosion Monitoring Technologies

- Schultz, C., S. Myers, J. Hipp, and C. Young (1998). Nonstationary Bayesian kriging; a predictive technique to generate spatial corrections for seismic detection, location, and identification, *Bull. Seismol. Soc. Am.* 88: 1275–1288.
- Wilson, D., D. Angus, J. Ni, and S. Grand (2006). Constraints on the interpretation of *S*-to-*P* receiver functions, *Geophys. J. Int.* 165: 969–980.
- Zhu, L. and L. Rivera (2002). A note on the dynamic and static displacements from a point source in multi-layered media, *Geophys. J. Int.* 148: 619–627.